Supplement of

Changes in the impacts of ship emissions on PM$_{2.5}$ and its components in China under the staged fuel oil policies

Guangyuan Yu et al.

Correspondence to: Yan Zhang (yan_zhang@fudan.edu.cn) and Cheng Huang (huangc@saes.sh.cn)
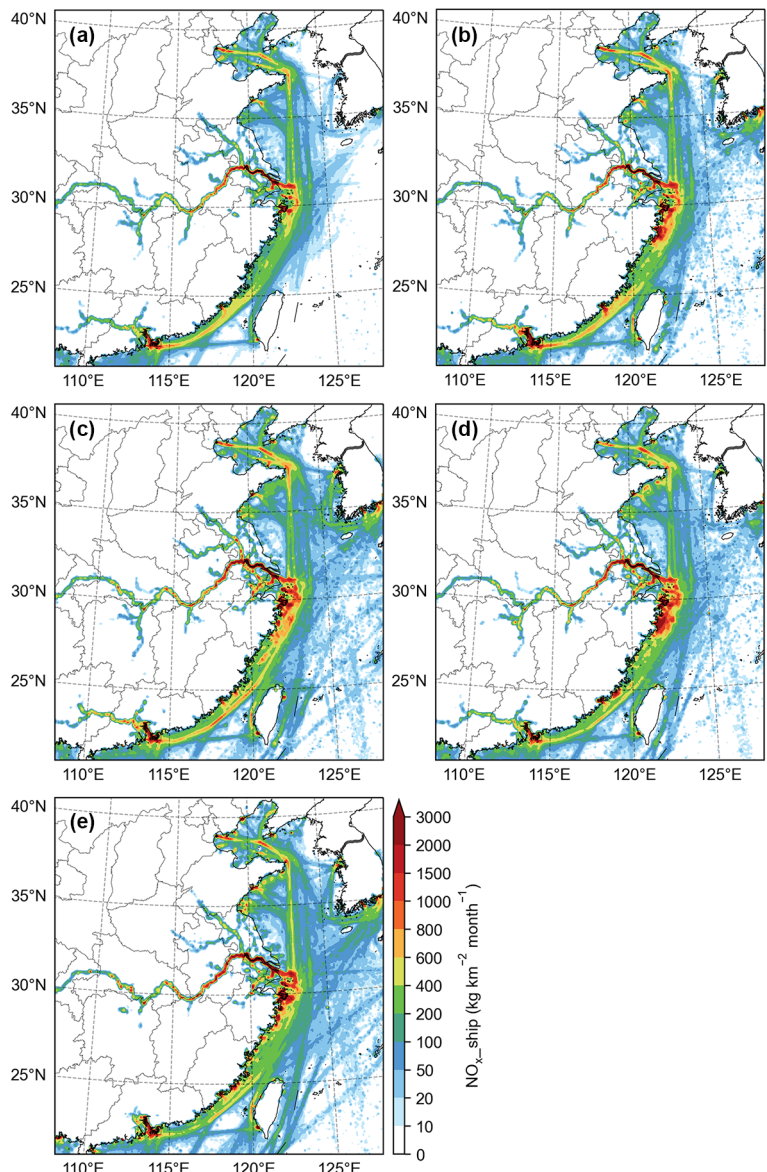
Figure S1. Spatial distribution of NO$_x$ emissions from shipping (NO$_x$_ship) in Domain 2 of the CMAQ model in **(a)** April 2017, **(b)** April 2018, **(c)** April 2019, **(d)** April 2020, and **(e)** April 2021.
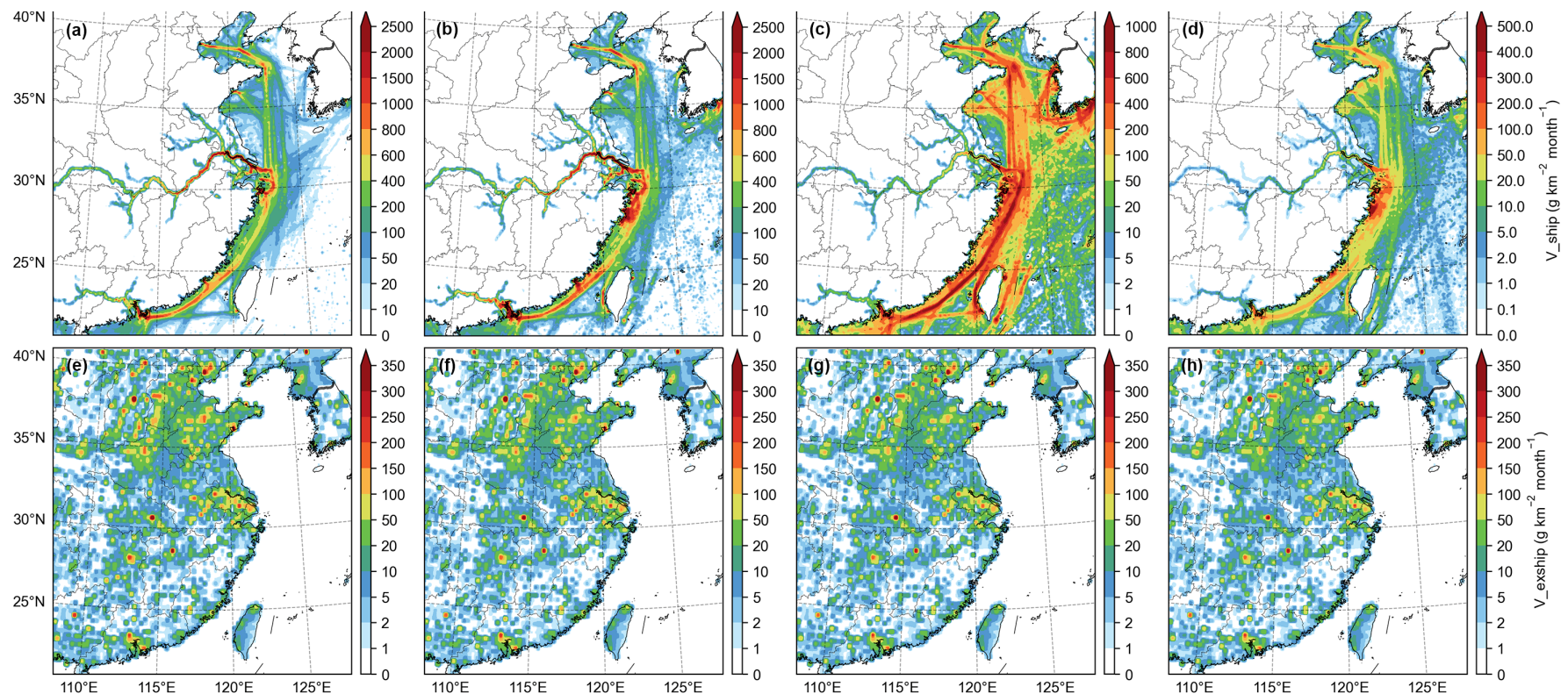
Figure S2. Spatial distribution of V emissions from shipping (V_ship) in **(a)** April 2017, **(b)** April 2018, **(c)** April 2019, and **(d)** April 2020; and spatial distribution of V emissions from anthropogenic sources excluding shipping (V_exship) in **(e)** April 2017, **(f)** April 2018, **(g)** April 2019, and **(h)** April 2020.
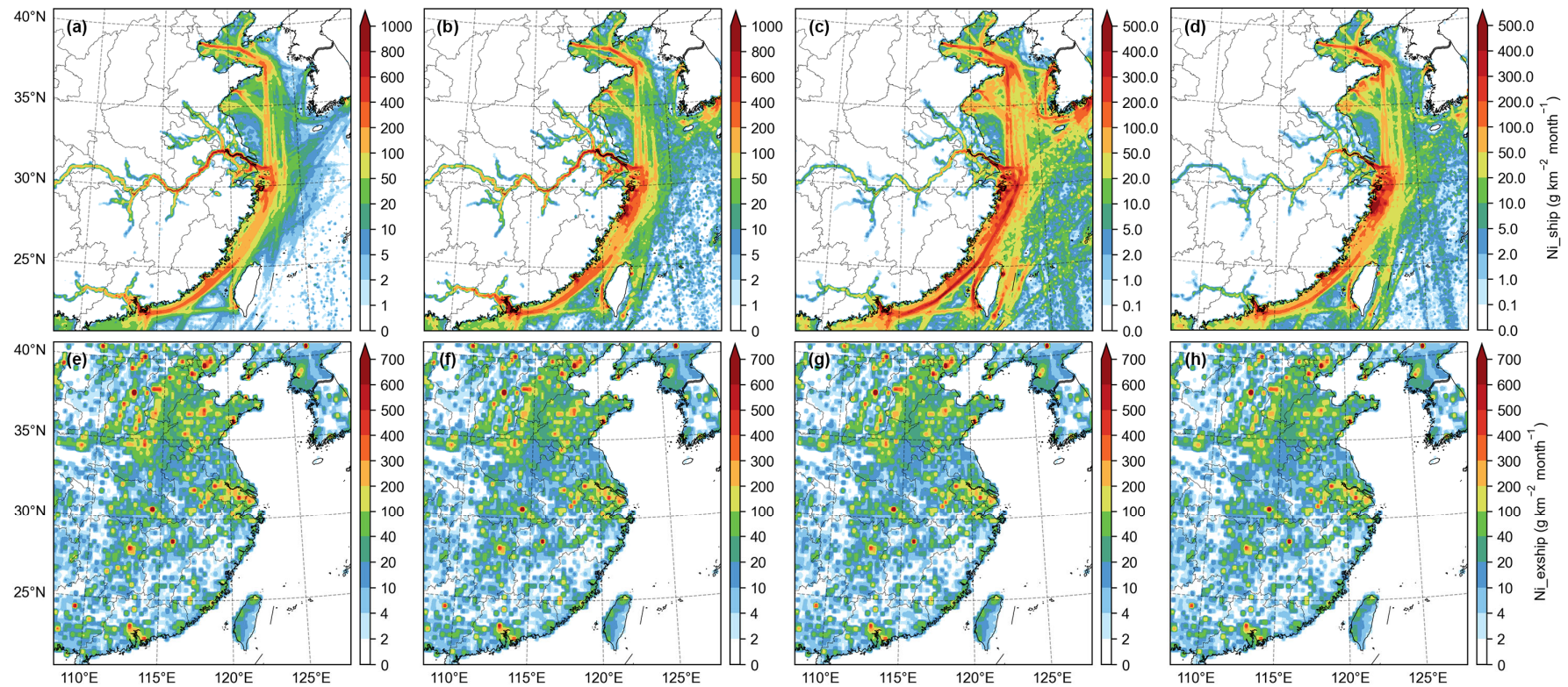
Figure S3. Spatial distribution of Ni emissions from shipping (Ni_ship) in **(a)** April 2017, **(b)** April 2018, **(c)** April 2019, and **(d)** April 2020; and spatial distribution of Ni emissions from anthropogenic sources excluding shipping (Ni_exship) in **(e)** April 2017, **(f)** April 2018, **(g)** April 2019, and **(h)** April 2020.
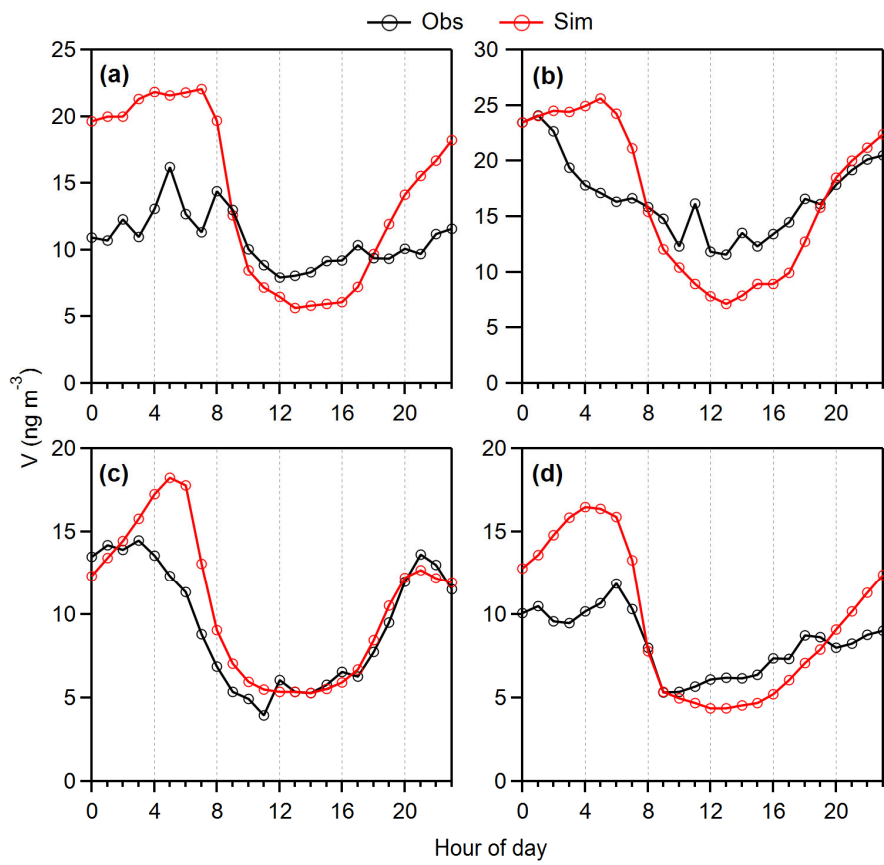
Figure S4. Comparison of observed (Obs) and simulated (Sim) diurnal variations of the V concentrations at the Pudong site of Shanghai in **(a)** January, **(b)** April, **(c)** July, and **(d)** October of 2017.
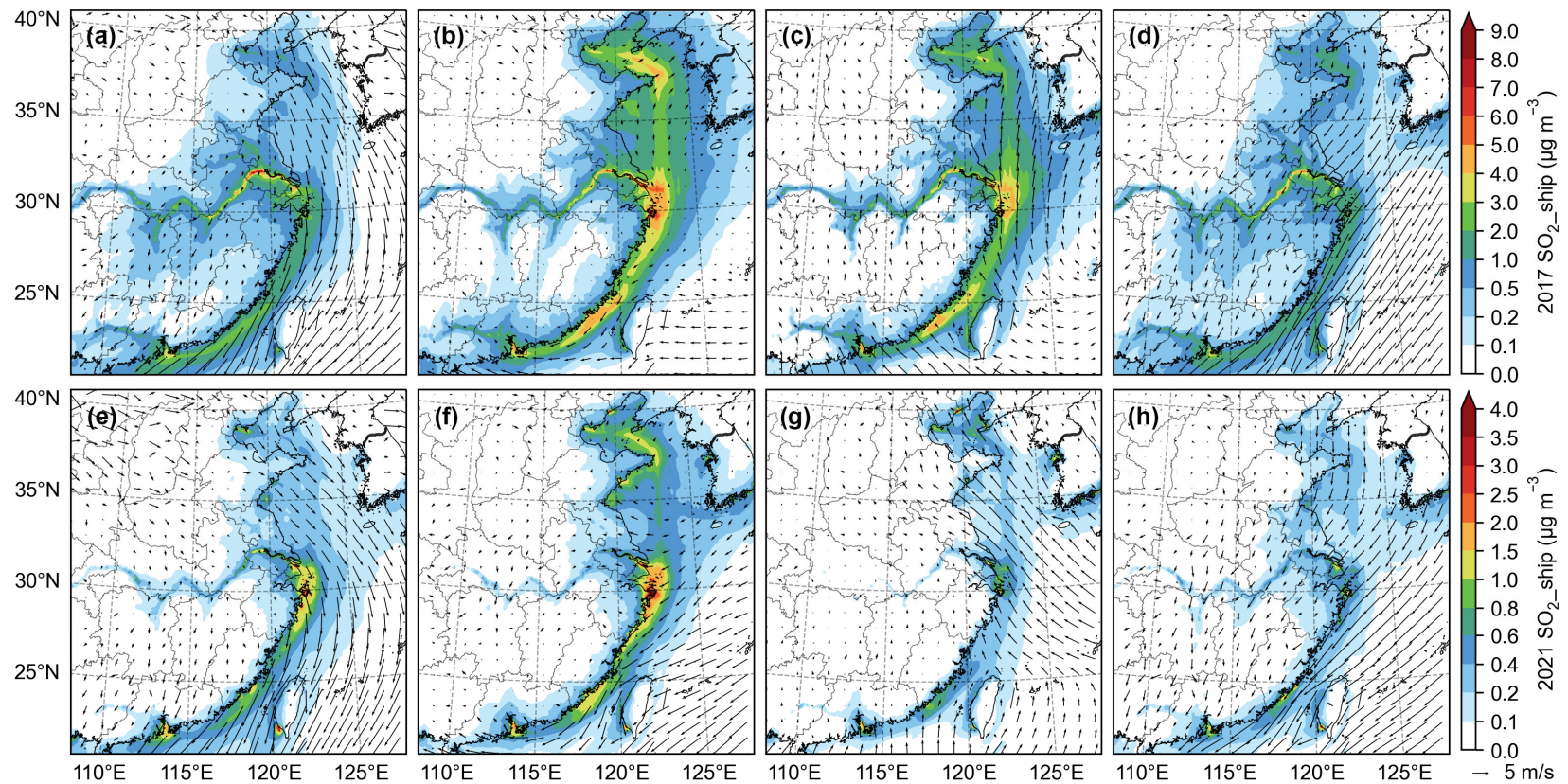
Figure S5. Seasonal variations of the impacts of ship emissions on the SO₂ concentrations (SO₂_ship) and simulated wind fields in **(a)** January 2017, **(b)** April 2017, **(c)** July 2017, **(d)** October 2017, **(e)** January 2021, **(f)** April 2021, **(g)** July 2021, and **(h)** October 2021.
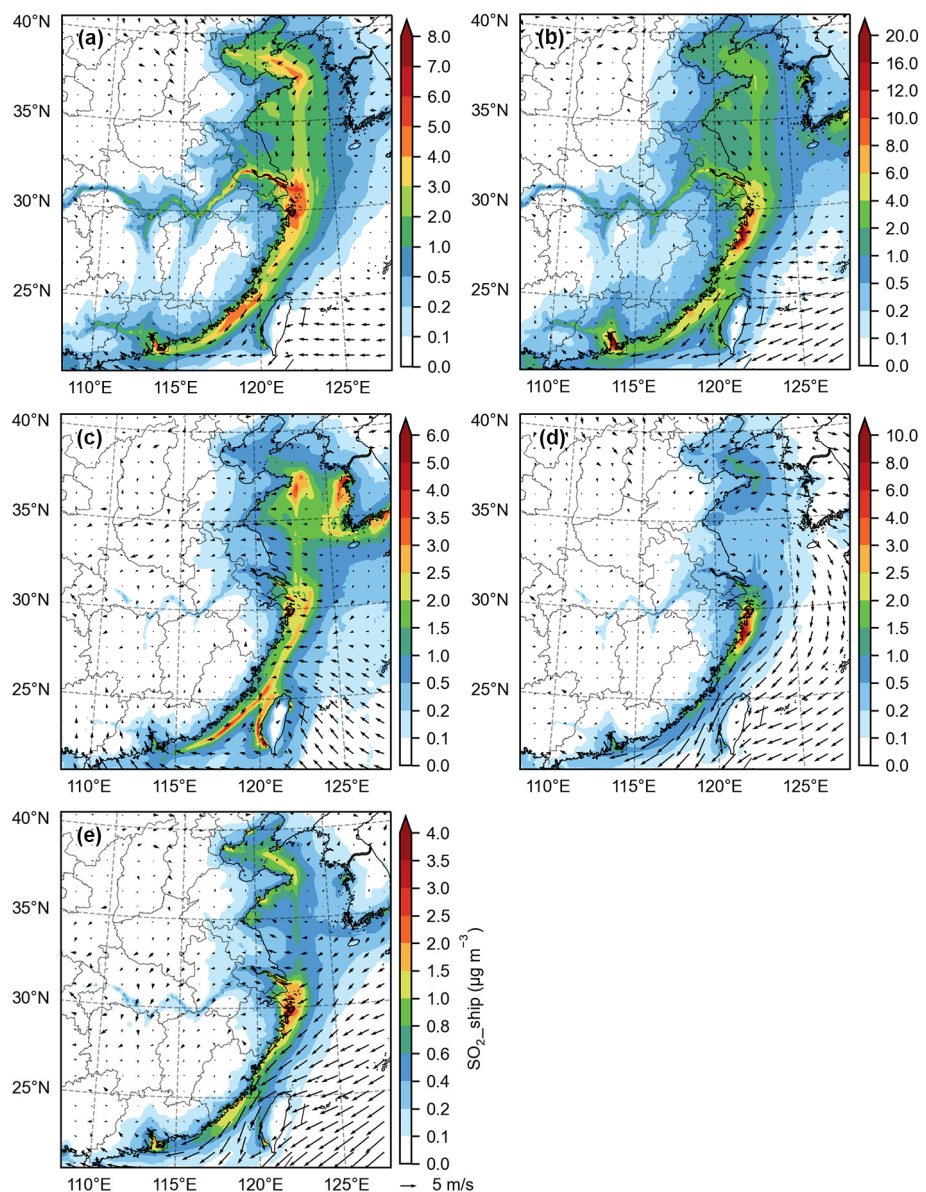
Figure S6. Impacts of ship emissions on the SO$_2$ concentrations (SO$_2$_ship) and simulated wind fields in April of **(a)** 2017, **(b)** 2018, **(c)** 2019, **(d)** 2020, and **(e)** 2021.
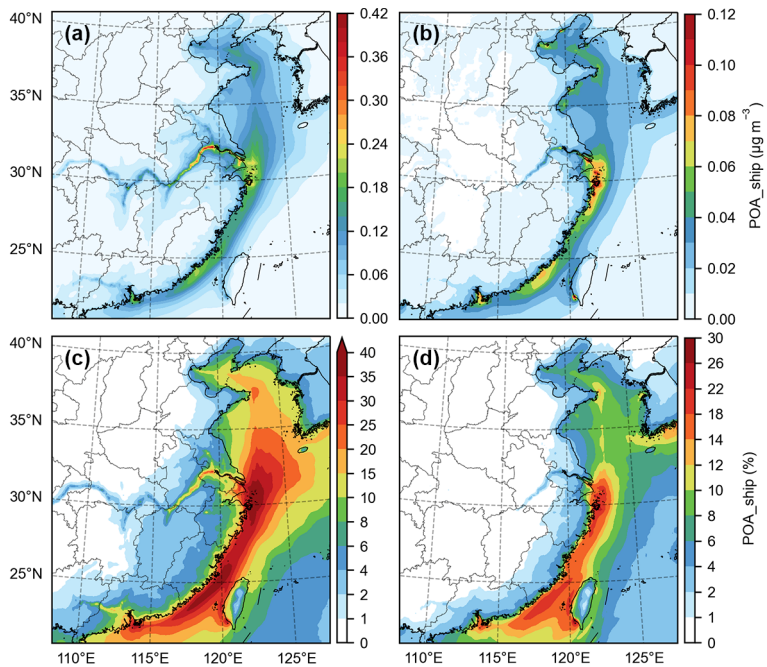
Figure S7. Impacts of ship emissions on primary organic aerosols (POA_ship): for concentration (in μg m^{-3}) in **(a)** 2017 and **(b)** 2021; and for contribution (in %) in **(c)** 2017 and **(d)** 2021.
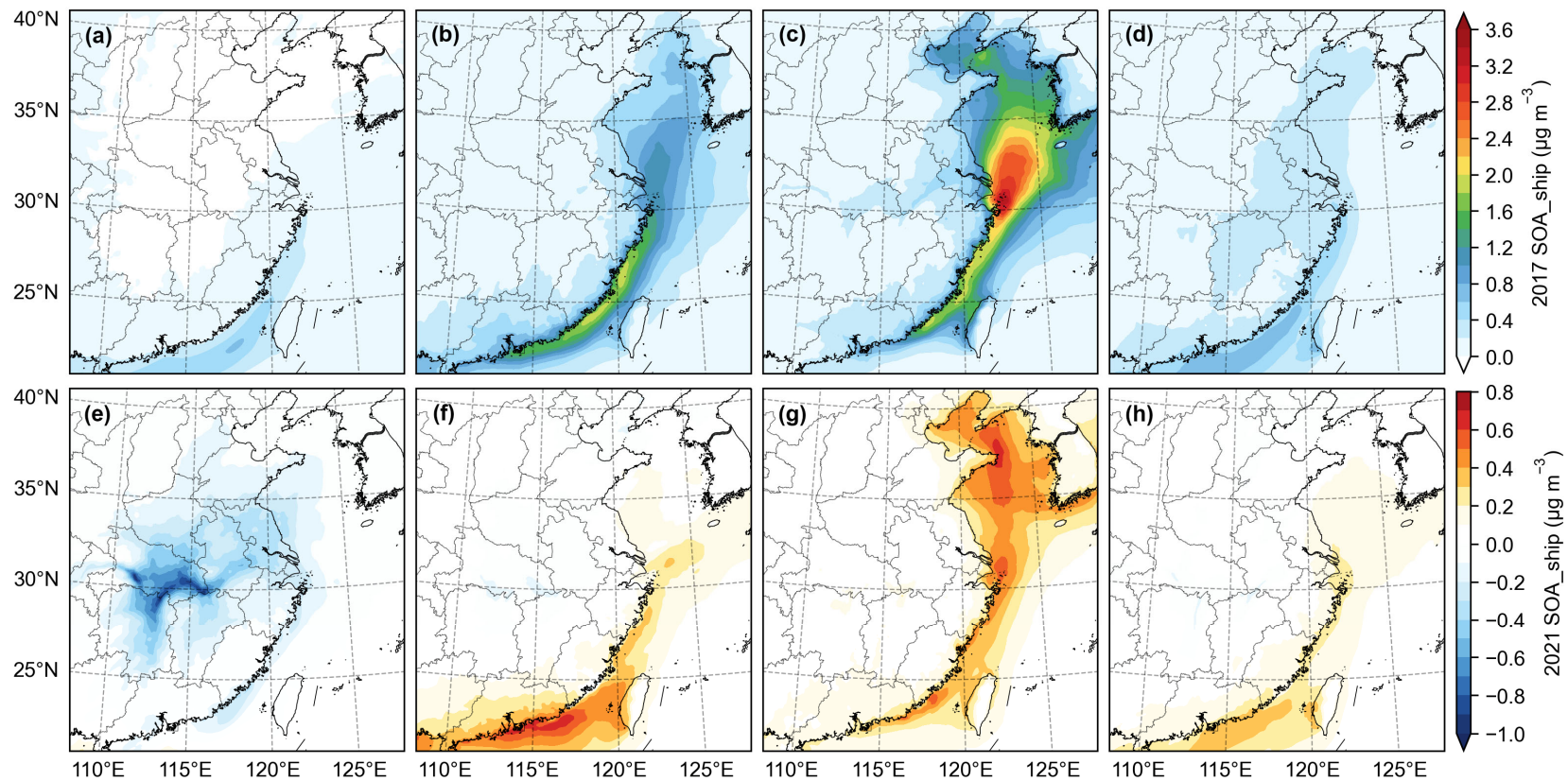
Figure S8. Seasonal variations of the potential impacts of ship emissions on secondary organic aerosols (SOA_ship) in **(a)** January 2017, **(b)** April 2017, **(c)** July 2017, **(d)** October 2017, **(e)** January 2021, **(f)** April 2021, **(g)** July 2021, and **(h)** October 2021.

Table S1. Power-based emissions factors of main engine (ME) and auxiliary engine (AE) (unit: g kWh^{-1}).

Engine type	Fuel type	SO$_2$	NO$_x$	CO	NMVOCs	PM$_{10}$	PM$_{2.5}$	NH$_3$	V	Ni
					For all areas in 2017–2018 and seas outside the CECA in 2019					
ME_SSD	HSFO	10.30	14.4	0.54	0.632	1.39	1.2788	4.90×10^{-3}	3.18×10^{-2}	1.03×10^{-2}
ME_MSD	HSFO	11.31	10.5	0.54	0.527	1.39	1.2788	2.90×10^{-3}	1.03×10^{-2}	3.51×10^{-3}
ME_HSD	MDO/MGO	0.42	7.7	0.54	0.527	0.18	0.1656	2.30×10^{-4}	4.25×10^{-5}	7.77×10^{-5}
AE	LSFO	2.12	11.2	0.54	0.421	0.73	0.6716	8.60×10^{-6}	5.42×10^{-4}	1.03×10^{-3}
					For the CECA in 2019					
ME_SSD	LSHFO	1.91	14.4	0.54	0.632	0.73	0.6716	4.90×10^{-3}	1.26×10^{-2}	1.03×10^{-2}
ME_MSD	LSHFO	2.09	10.5	0.54	0.527	0.73	0.6716	2.90×10^{-3}	4.10×10^{-3}	3.51×10^{-3}
ME_HSD	MDO/MGO	0.42	7.7	0.54	0.527	0.18	0.1656	2.30×10^{-4}	4.25×10^{-5}	7.77×10^{-5}
AE	ULSFO/ LSFO	1.25	11.2	0.54	0.421	0.46	0.4232	8.60×10^{-6}	2.15×10^{-4}	6.16×10^{-4}
					For sea areas in 2020–2021					
ME_SSD	LSHFO	1.91	14.4	0.54	0.632	0.73	0.6716	4.90×10^{-3}	3.18×10^{-3}	6.16×10^{-3}
ME_MSD	LSHFO	2.09	10.5	0.54	0.527	0.73	0.6716	2.90×10^{-3}	1.03×10^{-3}	2.10×10^{-3}
ME_HSD	MDO/MGO	0.42	7.7	0.54	0.527	0.18	0.1656	2.30×10^{-4}	4.25×10^{-5}	7.77×10^{-5}
AE	ULSFO/ LSFO	1.25	11.2	0.54	0.421	0.46	0.4232	8.60×10^{-6}	9.63×10^{-5}	5.54×10^{-4}

Note: ME and AE are main engine and auxiliary engine, respectively. SSD, MSD, and HSD are slow-speed diesel, medium-speed diesel, and high-speed diesel, respectively.

HSFO is high sulfur fuel oil with a sulfur content of ~2.7%. LSFO is low sulfur fuel oil with a sulfur content of ~0.5%. ULSFO is ultra-low sulfur fuel oil with a sulfur content of less than 0.1%. The sulfur content of marine diesel oil (MDO) and marine gas oil (MGO) is assumed to be ~0.1%.

Table S2. Source of emission factors of V and Ni from different sectors.

Engine type	Fuel type	Fuel sulfur content (%)	V (g kWh^{-1})	Ni (g kWh^{-1})	Reference
Power-based emission factors of V and Ni from shipping					
ME_SSD	HFO	2.85	1.99×10^{-2}	8.69×10^{-3}	Agrawal et al. (2008a)
		2.05	5.60×10^{-2}	1.27×10^{-2}	Agrawal et al. (2008b)
		2.70	1.94×10^{-2}	0.95×10^{-2}	Celo et al. (2015)
ME_MSD	HFO	2.70	1.43×10^{-2}	4.10×10^{-3}	Sippula et al. (2014)
		1.48	6.80×10^{-3}	2.43×10^{-3}	Celo et al. (2015)
		2.21	1.23×10^{-2}	0.55×10^{-2}	
		1.60	7.90×10^{-3}	2.00×10^{-3}	Streibel et al. (2017)
ME_HSD	MDO	0.08	4.25×10^{-5}	7.77×10^{-5}	Zhang et al. (2016)
AE_MSD	RME180 (LSFO)	0.412–0.501	1.89×10^{-4}	1.03×10^{-3}	Hou et al. (2023)
	MGO	0.0172–0.0461	3.52×10^{-6}	7.63×10^{-5}	

Sector	V (%)	Ni (%)	Reference
Mass fractions of V and Ni in PM$_{2.5}$ from other sources			
Industry	0.012	0.0265	Liu et al. (2018)
Power	0.019	0.050	
Residential	0.002	0.005	
Transportation	0.006	0.014	

Table S3. Mapping of PM$_{2.5}$ components to the AERO7 species.

Species	Industry	Power	Residential	Land-based transportation	Shipping (HSFO)	Shipping (LSHFO)
PAL	4.71×10^{-2}	5.26×10^{-2}	6.70×10^{-3}	3.45×10^{-2}	9.30×10^{-5}	2.17×10^{-2}
PCA	3.27×10^{-2}	2.56×10^{-2}	1.16×10^{-2}	1.04×10^{-2}	3.29×10^{-2}	3.29×10^{-2}
PCL	1.04×10^{-2}	1.48×10^{-2}	9.05×10^{-4}	6.90×10^{-3}	5.47×10^{-3}	9.25×10^{-4}
PEC	5.49×10^{-2}	3.16×10^{-2}	2.40×10^{-1}	1.01×10^{-1}	4.09×10^{-2}	6.98×10^{-2}
PFE	2.14×10^{-2}	3.34×10^{-2}	8.59×10^{-3}	1.89×10^{-2}	4.98×10^{-3}	6.71×10^{-3}
PK	3.60×10^{-3}	4.90×10^{-3}	5.33×10^{-3}	2.40×10^{-3}	8.38×10^{-4}	8.38×10^{-4}
PMG	1.11×10^{-2}	1.38×10^{-2}	2.90×10^{-3}	1.63×10^{-2}	8.71×10^{-4}	8.71×10^{-4}
PMN	8.40×10^{-4}	4.50×10^{-4}	1.50×10^{-4}	1.90×10^{-4}	5.03×10^{-4}	5.03×10^{-4}
PNA	3.00×10^{-3}	3.60×10^{-3}	2.02×10^{-4}	3.20×10^{-3}	6.19×10^{-3}	6.19×10^{-3}
PNCOM	4.40×10^{-2}	4.23×10^{-2}	1.79×10^{-1}	6.33×10^{-2}	1.42×10^{-1}	8.16×10^{-2}
PNH4	3.36×10^{-2}	2.69×10^{-2}	1.41×10^{-2}	7.90×10^{-3}	2.26×10^{-2}	2.29×10^{-2}
PNO3	2.26×10^{-2}	2.19×10^{-2}	3.15×10^{-3}	1.41×10^{-2}	1.27×10^{-2}	3.23×10^{-3}
POC	1.10×10^{-1}	1.06×10^{-1}	4.48×10^{-1}	2.53×10^{-1}	5.66×10^{-1}	3.26×10^{-1}
PSI	5.51×10^{-2}	5.94×10^{-2}	6.86×10^{-3}	3.45×10^{-2}	6.31×10^{-3}	5.03×10^{-2}
PSO4	1.93×10^{-1}	1.71×10^{-1}	3.32×10^{-2}	5.12×10^{-2}	1.17×10^{-1}	5.77×10^{-2}
PTI	2.20×10^{-3}	4.50×10^{-3}	4.00×10^{-4}	4.50×10^{-3}	1.89×10^{-5}	1.89×10^{-5}

Note: The profiles of industry, power, residential, and transportation sectors for PM$_{2.5}$ excluding V and Ni are obtained from Liu et al. (2017). The mass fractions before the IMO Regulation (2017−2019) and after 2020 were referenced from Huang et al. (2018a) and Yang et al. (2022), respectively.

Table S4. Convert factors of NMVOCs emissions from shipping to lumped species in the CB6 mechanism.

Species	Convert factor (mol kg^{-1})	Mass fraction
ACET	2.12	12.3%
ALD2	0.43	1.9%
ALDX	1.47	5.5%
BENZ	0.30	2.3%
ETH	0.57	1.6%
ETHA	0.14	0.4%
ETHY	0.47	1.2%
ETOH	0	0
FORM	0	0
IOLE	0.23	1.3%
ISOP	0.04	0.3%
KET	0.31	0.6%
MEOH	0	0
NAPH	0.25	3.2%
OLE	1.80	5.7%
PAR	20.83	30.2%
PRPA	0.15	0.7%
SOAALK	2.25 (0.108PAR)	-
TERP	0	0
TOL	1.83	16.9%
XYLMN	1.49	15.8%

Note: The convert factors were based on the median VOC profiles from the literature (Agrawal et al., 2008a; Huang et al., 2018b; Zhang et al., 2024).

Table S5. Vertical layer allocation of emission sectors for CMAQ input.

Layer	Height (m)	Shipping (marine)	Shipping (inland)	Land-based transportation	NH_3
1	0–50	20%	100%	100%	90%
2	50–109	80%	0	0	2%
3	109–179	0	0	0	6%
4	179–261	0	0	0	2%
5	261–358	0	0	0	0
6	358–472	0	0	0	0
7	472–603	0	0	0	0

Layer	Industry (VOCs)	Industry (except VOCs)	Power	Residential	Biogenic
1	50%	0	0	100%	100%
2	30%	20%	10%	0	0
3	16%	60%	10%	0	0
4	4%	20%	30%	0	0
5	0	0	20%	0	0
6	0	0	20%	0	0
7	0	0	10%	0	0

Note: The PKU-NH3 inventory in 2017 is used for non-shipping NH_3 in mainland China instead of the MEIC inventory.

Table S6. Detailed information on the studied cities and the monitoring sites.

Region	City	Port type	Latitude (cell center)	Longititude (cell center)	Meteorological station ID	Air quality monitoring station ID	Air quality data size
Bohai Bay	Dalian	Sea	38.923	121.601	54662	1109A, 1110A, 1011A, 1012A, 1013A	8038
	Yingkou	Sea	37.466	121.429	54471	1596A, 1597A, 1598A, 1599A	8057
	Caofeidian	Sea	39.229	118.403	54535	3457A	1817**
	Tianjin (downtown)*	Inland	39.141	117.185	54527	1015A, 1017A, 1018A, 1019A, 1021A, 2860A, 2922A	8032
	Tianjin (Binhai)	Estuary	39.057	117.739	54623	1023A	8030
	Yantai	Sea	40.619	122.243	54765	1643A, 1645A	8016
Yellow Sea	Qingdao	Sea	36.111	120.413	54857	1309A, 1310A, 1311A, 1312A, 1313A	8028
	Rizhao	Sea	35.437	119.442	54945	1659A, 1660A, 1661A, 3507A	8023
	Lianyungang	Sea	34.664	119.219	58040	1173A, 3434A, 3664A	7973
Yangtze River Delta	Shanghai	Estuary/ Sea/ Inland	31.217	121.437	58370	1141A, 1142A, 1143A, 1144A, 1145A, 1147A, 1148A, 1149A, 1150A, 3265A, 3268A, 3270A, 3271A, 3273A	8061
	Ningbo	Sea	29.877	121.634	58562	1234A, 1235A, 1236A, 1237A, 1239A, 1240A, 1241A, 2871A, 3710A	8064
	Zhoushan	Sea	30.029	122.236	58477	1258A, 1259A, 1260A	8064
	Hangzhou	Inland	30.257	120.155	58457	1223A, 1224A, 1227A, 1228A, 1230A	8036
	Nantong	Inland	32.05	120.911	58259	1168A, 1169A, 1170A, 1171A, 1172A, 3432A	8058
	Zhangjiagang	Inland	31.884	120.601	58353	1993A, 1994A	8061
	Nanjing	Inland	32.039	118.776	58238	1151A, 1152A, 1153A, 1154A, 1155A, 1156A, 1158A	8037
Fujian	Fuzhou	Estuary	26.067	119.297	58847	1282A, 1283A, 1284A, 1285A	8037
	Xiamen	Sea	24.54	118.153	59130	1287A, 1288A, 2842A, 3527A	8059
Pearl River Delta	Shenzhen	Estuary	22.602	114.025	59493	1356A, 1357A, 1358A, 1359A, 3305A, 3306A	8036
	Guangzhou	Estuary/ Inland	23.083	113.313	59287	1345A, 1346A, 1348A, 1349A, 1352A, 2846A, 3302A	8037
	Zhuhai	Estuary	26.1	123.771	59487	1367A, 1368A	8017
Beibu Gulf	Qinzhou	Sea	21.935	108.581	59632	2502A, 2503A, 2504A, 3404A	8064
Yantze River/ Central region	Wuhan*	Inland	30.649	114.262	57494	1325A, 1326A, 1327A, 1328A, 1331A, 1333A	8033
Northern region	Beijing*	-	39.905	116.396	54511	1001A, 1003A, 1004A, 1005A, 1006A, 1007A, 1011A	7987

* Tianjin (downtown), Wuhan, and Beijing are not included in the 21 representative port cities studied in this paper, and the observational data are only used in the evaluation of the model performance.

Table S7. Ship emissions in the 200-nm zone and the coastal provinces of Chinese mainland and their contributions to the total anthropogenic emissions in these areas.

Shipping	SO_2 (kt)	NO_x (kt)	CO (kt)	$PM_{2.5}$ (kt)	V (t)	Ni (t)
January 2017	42.9	102.9	4.6	7.3	122.6	42.4
April 2017	59.9	142.5	6.3	10.2	172.9	59.6
July 2017	58.0	133.9	5.7	9.5	163.1	56.0
October 2017	54.8	132.0	5.9	9.6	157.6	54.6
April 2018	86.6	199.7	8.8	14.5	249.1	85.6
April 2019	47.9	222.8	10.0	10.2	150.4	62.0
April 2020	20.0	212.8	9.6	7.8	23.1	47.3
January 2021	20.7	220.0	9.9	7.9	21.5	44.7
April 2021	20.8	216.7	9.7	7.9	21.2	44.2
July 2021	17.0	179.6	7.8	6.3	17.1	35.7
October 2021	20.1	216.6	9.9	7.7	20.5	42.9
2017 average per month	53.9	127.8	5.6	9.2	154.0	53.1
2021 average per month	19.6	208.2	9.3	7.4	20.1	41.9
Contribution of shipping	SO_2 (%)	NO_x (%)	CO (%)	$PM_{2.5}$ (%)	V (%)	Ni (%)
January 2017	10.4	11.3	0.1	2.7	87.0	50.1
April 2017	15.6	14.6	0.2	4.8	90.0	57.8
July 2017	15.0	13.5	0.1	4.5	89.6	56.5
October 2017	14.7	13.5	0.2	4.6	89.6	56.7
April 2018	24.4	19.5	0.2	7.3	93.5	68.6
April 2019	16.7	21.9	0.3	5.5	90.2	62.6
April 2020	8.4	22.4	0.3	4.6	60.4	58.0
January 2021	7.3	22.3	0.2	3.5	57.0	54.6
April 2021	8.8	22.7	0.3	4.6	58.4	56.3
July 2021	7.0	18.6	0.2	3.7	52.1	50.0
October 2021	8.0	21.3	0.3	4.3	56.0	54.0
2017 average	13.9	13.2	0.1	4.0	89.2	55.5
2021 average	7.7	21.2	0.3	4.0	56.0	53.8

Note: The anthropogenic emissions from sources excluding shipping are obtained from the MEIC inventory, and their values in 2020 (the latest year of the MEIC) are used to represent those in 2021.

Table S8. Comparison of hourly meteorological elements between simulated results and observational data.

City	2-m temperature (°C)				Relative humidity (%)				10-m wind speed (m s⁻¹)				10-m wind direction (°)	
	$\overline{Obs}$	$\overline{Sim}$	r	NMB	$\overline{Obs}$	$\overline{Sim}$	r	NMB	$\overline{Obs}$	$\overline{Sim}$	r	NMB	$\overline{Obs}$	$\overline{Sim}$
Shanghai	17.79	17.75	0.97	-0.2%	73.2	66.6	0.78	-9.0%	2.22	4.34	0.51	95.5%	87.7	96.5
Ningbo	18.38	18.39	0.97	0.1%	72.1	68.5	0.75	-5.0%	3.35	3.85	0.53	15.0%	31.3	110.2
Zhoushan	17.60	16.61	0.96	-5.6%	78.6	78.1	0.73	-0.7%	3.26	4.06	0.43	24.4%	47.8	92.7
Nantong	16.94	17.60	0.97	3.9%	75.5	62.8	0.80	-16.8%	3.81	4.20	0.61	10.4%	74.6	81.5
Zhangjiagang	17.49	18.01	0.97	3.0%	70.7	60.7	0.79	-14.1%	2.99	4.12	0.51	37.8%	61.3	81.0
Nanjing	17.31	17.92	0.97	3.5%	70.4	58.5	0.80	-17.0%	3.34	3.99	0.51	19.3%	73.5	81.6
Hangzhou	18.61	19.14	0.96	2.8%	68.1	58.5	0.76	-14.2%	3.08	3.49	0.46	13.3%	5.2	48.4
Fuzhou	21.17	20.99	0.95	-0.9%	70.2	65.2	0.60	-7.1%	2.96	2.69	0.41	-9.1%	67.4	62.6
Xiamen	22.53	22.30	0.94	-1.1%	71.4	64.4	0.69	-9.8%	2.65	3.62	0.56	36.6%	89.2	59.0
Guangzhou	22.25	23.93	0.91	7.5%	78.3	62.3	0.68	-20.4%	2.66	4.08	0.49	53.1%	1.9	88.8
Shenzhen	23.52	23.58	0.91	0.3%	75.4	68.6	0.75	-9.1%	2.59	4.46	0.48	72.2%	62.1	87.7
Zhuhai	23.62	23.90	0.90	1.2%	79.5	70.3	0.74	-11.6%	2.65	4.20	0.48	58.3%	85.8	94.8
Qinzhou	22.60	22.99	0.88	1.8%	82.2	72.7	0.72	-11.6%	3.94	3.96	0.56	0.6%	6.2	35.3
Tianjin (downtown)	14.01	14.56	0.97	3.9%	56.2	44.4	0.78	-20.9%	3.51	3.87	0.58	10.3%	142.9	203.2
Tianjin (Binhai)	13.97	13.56	0.97	-2.9%	56.1	51.0	0.76	-9.1%	3.47	4.45	0.56	28.2%	155.2	160.7
Caofeidian	12.84	12.52	0.97	-2.5%	62.3	51.9	0.77	-16.8%	3.26	4.33	0.60	32.6%	206.3	218.3
Yingkou	10.84	10.65	0.98	-1.7%	61.6	56.6	0.72	-8.2%	4.26	4.88	0.58	14.4%	238.0	238.8
Dalian	11.96	11.64	0.98	-2.7%	58.8	60.2	0.82	2.4%	4.03	4.70	0.57	16.8%	312.5	282.4
Yantai	13.12	13.15	0.98	0.2%	62.0	60.7	0.78	-2.0%	4.81	4.73	0.58	-1.6%	291.2	280.7
Qingdao	13.54	13.56	0.98	0.1%	67.9	62.5	0.78	-7.9%	4.59	4.45	0.58	-2.9%	80.2	97.5
Rizhao	14.04	14.27	0.97	1.7%	67.6	60.0	0.77	-11.2%	4.21	4.03	0.54	-4.3%	32.2	31.7
Lianyungang	14.84	15.18	0.96	2.3%	70.8	60.8	0.74	-14.1%	3.46	4.35	0.61	25.8%	68.8	66.8
Wuhan	17.70	18.31	0.96	3.4%	76.4	61.2	0.66	-19.8%	2.38	3.60	0.56	51.1%	30.0	34.8
Xi'an	14.95	16.58	0.96	10.9%	64.6	46.6	0.72	-27.8%	2.63	3.22	0.41	22.5%	44.3	33.4
Beijing	13.98	14.66	0.97	4.9%	52.1	40.5	0.77	-22.4%	2.76	3.37	0.54	22.0%	297.9	256.1

Note:$\overline{Obs}$ and $\overline{Sim}$ are mean values of observational data and simulated results, respectively. The hourly wind direction observational data of Guangzhou started in 2018.

Table S9. Comparison of the concentrations of the main air pollutants in the studied cities between simulated results and observational data.

City	SO_2 ($\mu g\ m^{-3}$)				NO_2 ($\mu g\ m^{-3}$)				MDA8 O_3 ($\mu g\ m^{-3}$)				$PM_{2.5}$ ($\mu g\ m^{-3}$)			
	$\overline{Obs}$	$\overline{Sim}$	r	NMB	$\overline{Obs}$	$\overline{Sim}$	r	NMB	$\overline{Obs}$	$\overline{Sim}$	r	NMB	$\overline{Obs}$	$\overline{Sim}$	r	NMB
Shanghai	8.9	15.9	0.48	79.0%	39.5	64.5	0.58	63.2%	108.9	79.9	0.76	-26.6%	33.2	24.4	0.55	-26.6%
Ningbo	9.2	6.0	0.51	-34.5%	33.8	39.6	0.51	16.7%	102.4	91.5	0.60	-10.7%	27.6	19.2	0.54	-30.7%
Zhoushan	7.1	4.0	0.51	-43.9%	18.9	23.1	0.45	22.3%	100.0	89.3	0.53	-10.7%	19.8	14.5	0.50	-26.9%
Nantong	13.5	8.3	0.51	-38.6%	33.0	38.5	0.58	16.3%	109.8	92.4	0.68	-15.8%	35.4	22.7	0.56	-35.8%
Zhangjiagang	10.9	9.2	0.29	-15.3%	37.5	46.5	0.52	23.9%	107.3	89.9	0.71	-16.4%	36.4	24.4	0.58	-33.0%
Nanjing	11.4	10.0	0.33	-12.1%	42.0	51.5	0.52	22.5%	108.4	89.5	0.65	-17.5%	35.4	30.2	0.57	-14.5%
Hangzhou	8.3	7.3	0.42	-12.1%	40.6	44.5	0.45	9.5%	104.1	99.7	0.74	-4.2%	35.5	24.0	0.51	-32.4%
Fuzhou	5.8	3.8	0.24	-34.0%	26.6	21.0	0.37	-21.1%	97.0	100.4	0.55	3.5%	26.0	14.5	0.35	-44.3%
Xiamen	8.3	6.2	0.40	-25.6%	25.8	36.7	0.35	41.9%	90.7	94.4	0.51	4.1%	24.7	19.9	0.40	-19.5%
Guangzhou	9.7	9.1	0.46	-5.9%	50.9	43.6	0.37	-14.4%	97.4	102.3	0.54	5.1%	31.8	18.0	0.44	-43.4%
Shenzhen	6.5	11.0	0.26	67.8%	29.5	45.6	0.37	54.5%	89.8	85.0	0.58	-5.4%	24.1	16.0	0.52	-33.6%
Zhuhai	5.8	4.8	0.32	-16.3%	30.4	20.0	0.48	-34.2%	92.5	104.0	0.54	12.3%	23.5	13.4	0.50	-42.8%
Qinzhou	13.8	3.1	0.27	-77.6%	19.0	5.3	0.28	-72.2%	83.1	99.9	0.51	20.1%	32.0	16.6	0.58	-48.4%
Tianjin (downtown)	11.9	14.8	0.49	24.5%	42.3	61.8	0.58	46.1%	105.1	65.1	0.78	-38.1%	52.8	32.9	0.58	-37.6%
Tianjin (Binhai)	11.8	8.1	0.34	-31.7%	52.4	35.3	0.50	-32.9%	89.0	79.7	0.71	-10.4%	50.9	28.1	0.59	-44.9%
Caofeidian	9.0	5.4	0.21	-39.8%	27.2	23.3	0.60	-14.1%	106.1	92.7	0.69	-12.7%	33.3	23.5	0.60	-29.2%
Yingkou	12.8	6.7	0.56	-47.4%	29.2	23.8	0.54	-18.4%	110.4	81.3	0.64	-26.3%	41.1	23.7	0.54	-42.2%
Dalian	12.4	10.4	0.42	-16.3%	29.1	43.9	0.40	51.1%	105.7	70.0	0.58	-33.8%	31.7	27.4	0.53	-13.6%
Yantai	13.6	7.2	0.39	-47.1%	30.8	25.2	0.52	-18.1%	106.7	85.4	0.52	-20.0%	30.9	25.2	0.60	-18.6%
Qingdao	11.6	12.7	0.60	9.5%	33.8	43.4	0.55	28.2%	107.1	76.7	0.52	-28.4%	33.4	30.7	0.56	-8.0%
Rizhao	10.6	7.2	0.56	-32.0%	33.8	24.7	0.53	-26.9%	103.6	89.8	0.62	-13.4%	41.6	28.9	0.62	-30.9%
Lianyungang	14.3	4.9	0.54	-65.5%	28.4	20.1	0.52	-29.1%	108.2	93.8	0.57	-13.3%	40.2	27.0	0.59	-32.7%
Wuhan	8.4	24.1	0.44	187.8%	42.1	44.3	0.53	5.4%	94.0	94.5	0.67	0.5%	40.7	43.3	0.65	6.5%
Xi'an	11.7	10.6	0.68	-9.5%	50.9	33.6	0.36	-34.0%	90.8	87.9	0.77	-3.2%	55.9	29.7	0.62	-46.7%
Beijing	5.6	9.3	0.48	69.1%	40.0	66.5	0.53	66.2%	97.4	69.3	0.76	-28.8%	49.7	34.6	0.58	-30.2%

Note: The concentrations of SO_2, NO_2, and $PM_{2.5}$ are in hourly resolution. The daily maximum 8-h average (MDA8) O_3 concentrations are in daily resolution. The observational data from Caofeidian started from 17 April 2021.

Table S10. Comparison of the hourly concentrations of sulfate, nitrate, and ammonium between simulated results and observational data at the Pudong site of Shanghai.

SNA	Parameter	Jan. 2017	Apr. 2017	Jul. 2017	Oct. 2017	Apr. 2018	Apr. 2019	Apr. 2020	Jan. 2021	Apr. 2021	Jul. 2021	Oct. 2021
SO_4^{2-}	N (obs)	707	702	691	693	693	557	673	691	707	738	706
	N (sim)	744	720	744	744	720	720	720	744	720	744	744
	Obs ($\mu g\ m^{-3}$)	9.47	8.06	5.96	4.83	6.82	6.21	4.33	5.13	4.71	3.41	3.37
	Sim ($\mu g\ m^{-3}$)	6.62	7.02	5.12	3.87	4.99	6.02	4.01	5.00	4.21	2.71	3.13
	r	0.41	0.10	0.71	0.30	0.33	0.04	0.03	0.19	0.32	0.34	0.25
	NMB (%)	-30.4	-12.1	-15.4	-19.3	-25.7	-1.8	-6.9	-3.0	-10.1	-20.2	-6.2
	RMSE ($\mu g\ m^{-3}$)	7.33	6.48	2.73	3.94	4.34	6.41	3.22	3.61	4.92	2.27	2.60
NO_3^-	N (obs)	707	702	691	691	693	557	673	691	707	738	706
	N (sim)	744	720	744	744	720	720	720	744	720	744	744
	Obs ($\mu g\ m^{-3}$)	11.42	10.45	2.58	4.11	8.73	11.62	8.30	9.08	8.59	2.46	3.59
	Sim ($\mu g\ m^{-3}$)	14.56	5.48	1.71	1.94	5.26	9.27	5.88	14.38	5.17	1.30	3.05
	r	0.61	0.36	0.54	0.33	0.38	0.46	0.27	0.26	0.52	0.34	0.65
	NMB (%)	26.0	-47.4	-33.3	-51.1	-41.2	-16.0	-29.0	63.8	-39.0	-46.8	-7.8
	RMSE ($\mu g\ m^{-3}$)	11.00	9.28	4.45	5.61	9.02	11.00	7.48	12.42	8.88	5.01	5.67
NH_4^+	N (obs)	707	702	675	686	692	556	673	691	707	730	706
	N (sim)	744	720	744	744	720	720	720	744	720	744	744
	Obs ($\mu g\ m^{-3}$)	7.48	5.91	3.15	2.63	4.70	5.49	3.93	5.50	4.16	1.88	1.99
	Sim ($\mu g\ m^{-3}$)	6.20	6.35	2.00	1.51	2.77	4.53	2.60	5.45	2.44	0.90	1.51
	r	0.65	0.47	0.67	0.35	0.38	0.43	0.22	0.20	0.52	0.43	0.77
	NMB (%)	-17.9	9.1	-36.6	-41.2	-41.6	-14.5	-33.0	0.9	-40.6	-51.5	-23.1
	RMSE ($\mu g\ m^{-3}$)	4.86	6.02	2.21	2.97	3.99	4.42	3.24	4.07	3.95	2.06	1.66

Note: N(obs) and N (sim) are numbers of observational data and simulated results, respectively.

Table S11. Comparison of hourly V and Ni concentration between simulated results and observational data at the Pudong site of Shanghai during the simulation period.

Metal	Parameter	Jan. 2017	Apr. 2017	Jul. 2017	Oct. 2017	Apr. 2018	Apr. 2019	Apr. 2020	Jan. 2021	Apr. 2021	Jul. 2021	Oct. 2021
V	N (obs)	679	623	596	733	567	503	281	233	374	394	361
	N (sim)	744	720	744	744	720	720	720	744	720	744	744
	$\overline{Obs}$ (ng m^{-3})	10.76	17.02	9.70	8.27	16.32	7.23	1.23	1.49	1.41	1.46	1.11
	$\overline{Sim}$ (ng m^{-3})	15.18	17.65	11.08	9.93	15.81	7.73	2.21	2.41	1.86	0.90	1.43
	r	0.43	0.12	0.61	0.29	0.33	0.56	0.41	0.35	0.24	0.25	0.13
	IoA	0.63	0.41	0.75	0.48	0.51	0.73	0.54	0.53	0.47	0.48	0.41
	RMSE (ng m^{-3})	14.22	22.40	10.00	12.49	16.83	7.22	2.14	2.21	1.73	1.23	1.47
Ni	N (obs)	741	714	714	735	612	608	703	743	701	621	738
	N (sim)	744	720	744	744	720	720	720	744	720	744	744
	$\overline{Obs}$ (ng m^{-3})	5.08	7.21	4.60	4.45	7.64	5.39	3.59	3.72	3.88	2.92	3.47
	$\overline{Sim}$ (ng m^{-3})	6.83	7.02	4.56	3.91	6.01	4.22	4.14	4.84	3.37	1.81	2.90
	r	0.33	0.17	0.59	0.21	0.30	0.45	0.28	0.27	0.31	0.26	0.42
	IoA	0.56	0.44	0.76	0.44	0.46	0.58	0.50	0.49	0.58	0.48	0.65
	RMSE (ng m^{-3})	5.46	7.53	3.42	5.04	6.70	5.02	3.54	4.12	3.06	2.36	2.62
Ni/V	$\overline{Obs}$	0.47	0.42	0.47	0.54	0.47	0.75	2.92	2.50	2.74	2.00	3.14
	$\overline{Sim}$	0.45	0.40	0.41	0.39	0.38	0.55	1.87	2.01	1.82	2.01	2.03

Note: N(obs) and N (sim) are numbers of observational data and simulated results, respectively.

References

Agrawal, H., Welch, W. A., Miller, J. W., and Cocker, D. R.: Emission Measurements from a Crude Oil Tanker at Sea, Environmental Science & Technology, 42, 7098-7103, https://doi.org/10.1021/es703102y, 2008a.

Agrawal, H., Malloy, Q. G. J., Welch, W. A., Wayne Miller, J., and Cocker, D. R.: In-use gaseous and particulate matter emissions from a modern ocean going container vessel, Atmospheric Environment, 42, 5504-5510, https://doi.org/10.1016/j.atmosenv.2008.02.053, 2008b.

Celo, V., Dabek-Zlotorzynska, E., and McCurdy, M.: Chemical characterization of exhaust emissions from selected canadian marine vessels: the case of trace metals and lanthanoids, Environmental Science & Technology, 49, 5220-5226, https://doi.org/10.1021/acs.est.5b00127, 2015.

Hou, W., Liu, Z., Yu, G., Bie, S., Zhang, Y., Chen, Y., Ma, D., Zhang, F., Lou, C., Hu, X., Gui, Y., and Zhou, W.: On-board measurements of OC/EC ratio, mixing state, and light absorption of ship-emitted particles, Science of the Total Environment, 904, 166692, https://doi.org/10.1016/j.scitotenv.2023.166692, 2023.

Huang, C., Hu, Q., Wang, H., Qiao, L., Jing, S., Wang, H., Zhou, M., Zhu, S., Ma, Y., Lou, S., Li, L., Tao, S., Li, Y., and Lou, D.: Emission factors of particulate and gaseous compounds from a large cargo vessel operated under real-world conditions, Environmental Pollution, 242, 667-674, https://doi.org/10.1016/j.envpol.2018.07.036, 2018a.

Huang, C., Hu, Q., Li, Y., Tian, J., Ma, Y., Zhao, Y., Feng, J., An, J., Qiao, L., Wang, H., Jing, S., Huang, D., Lou, S., Zhou, M., Zhu, S., Tao, S., and Li, L.: Intermediate Volatility Organic Compound Emissions from a Large Cargo Vessel Operated under Real-World Conditions, Environmental Science & Technology, 52, 12934-12942, https://doi.org/10.1021/acs.est.8b04418, 2018b.

Yang, L., Zhang, Q., Zhang, Y., Lv, Z., Wu, L., and Mao, H.: Real-world emission characteristics of an ocean-going vessel through long sailing measurement, Science of the Total Environment, 810, 152276, https://doi.org/10.1016/j.scitotenv.2021.152276, 2022.

Liu, Y., Xing, J., Wang, S., Fu, X., and Zheng, H.: Source-specific speciation profiles of $PM_{2.5}$ for heavy metals and their anthropogenic emissions in China, Environmental Pollution, 239, 544-553, https://doi.org/10.1016/j.envpol.2018.04.047, 2018.

Liu, Y., Zhang, W., Bai, Z., Yang, W., Zhao, X., Han, B., and Wang, X.: China Source Profile Shared Service (CSPSS): The Chinese $PM_{2.5}$ Database for Source Profiles, Aerosol and Air Quality Research, 17, 1501-1514, https://doi.org/10.4209/aaqr.2016.10.0469, 2017.

Sippula, O., Stengel, B., Sklorz, M., Streibel, T., Rabe, R., Orasche, J., Lintelmann, J., Michalke, B., Abbaszade, G., Radischat, C., Groger, T., Schnelle-Kreis, J., Harndorf, H., and Zimmermann, R.: Particle emissions from a marine engine: chemical composition and aromatic emission profiles under various operating conditions, Environmental Science & Technology, 48, 11721-11729, https://doi.org/10.1021/es502484z, 2014.

Streibel, T., Schnelle-Kreis, J., Czech, H., Harndorf, H., Jakobi, G., Jokiniemi, J., Karg, E., Lintelmann, J., Matuschek, G., Michalke, B., Muller, L., Orasche, J., Passig, J., Radischat, C., Rabe, R., Reda, A., Ruger, C., Schwemer, T., Sippula, O., Stengel, B., Sklorz, M., Torvela, T., Weggler, B., and Zimmermann, R.: Aerosol emissions of a ship diesel engine operated with diesel fuel or heavy fuel oil, Environmental Science and Pollution Research, 24, 10976-10991, https://doi.org/10.1007/s11356-016-6724-z, 2017.

Zhang, F., Chen, Y., Tian, C., Lou, D., Li, J., Zhang, G., and Matthias, V.: Emission factors for gaseous and particulate pollutants from offshore diesel engine vessels in China, Atmospheric Chemistry and Physics, 16, 6319-6334, https://doi.org/10.5194/acp-16-6319-2016, 2016.

Zhang, F., Xiao, B., Liu, Z., Zhang, Y., Tian, C., Li, R., Wu, C., Lei, Y., Zhang, S., Wan, X., Chen, Y., Han, Y., Cui, M., Huang, C., Wang, H., Chen, Y., and Wang, G.: Real-world emission characteristics of VOCs from typical cargo ships and their potential contributions to secondary organic aerosol and O3 under low-sulfur fuel policies, Atmospheric Chemistry and Physics, 24, 8999-9017, https://doi.org/10.5194/acp-24-8999-2024, 2024.